Avrupa Bilim ve Teknoloji Dergisi
Özel Sayı 37, S. 28-35, Haziran 2022

Araştırma Makalesi

www.ejosat.com ISSN:2148-2683

European Journal of Science and Technology
Special Issue 37, pp. 28-35, June 2022

Research Article

Feedback Linearization Based Flow Rate Control for Centrifugal Pump in Coupled-Tank Water Meter Testing System

Bahadır Yeşil[1, 2*], Savaş Şahin[3]

[1] İzmir Katip Çelebi Üniversitesi, Fen Bilimleri Enstitüsü, Elektrik-Elektronik Mühendisliği Ana Bilim Dalı, İzmir, Türkiye, (ORCID: 0000-0002-9622-2593),
[2] Baylan Ölçü Aletleri Sanayi ve Ticaret Limited Şirketi, Arge Merkezi, İzmir, Türkiye, b.yesil@baylanwatermeters.com
[3] İzmir Katip Çelebi Üniversitesi, Mühendislik Fakültesi, Elektrik-Elektronik Mühendisliği Bölümü, İzmir, Türkiye, (ORCID: 0000-0003-2065-6907), phd.savas.sahin@gmail.com

(5th International Symposium on Innovative Approaches in Smart Technologies– 28-29 May 2022)

(**DOI:** 10.31590/ejosat.1128945)

ATIF/REFERENCE: Yeşil, B. & Şahin, S. (2022). Feedback Linearization Based Flow Rate Control for Centrifugal Pump in Coupled-Tank Water Meter Testing System. *European Journal of Science and Technology*, (37), 28-35.

Abstract

A permanent magnet direct current (PMDC) motor centrifugal pump is intended to be used as the water supply unit in a feedback linearization based coupled-tank water meter testing system. Flow rate generated by the pump corresponds to the input variable for implementing the input-output feedback linearization to this single-input-single-output (SISO) system. The pump motor is driven by an Arm Cortex M7 based microcontroller applying the pulse-width modulation (PWM) strategy at various frequencies and pwm methods. It is aimed to determine a suitable PWM frequency and driving method in order to provide a stable flow rate at the desired duty cycle values. An H-Bridge driver integrated circuit (L298N) is used in both fast decay and slow decay modes for driving the pump motor. Flow rate measurements are carried out at 4 range of frequencies between 100 Hz and 20 kHz for each mode. Fast decay mode in low pwm frequency (100Hz) results in higher deviations at the steady-state flow rate. However, slow decay mode provides a faster reduction in motor speed despite the slower current decay, which improves the flow rate stability and minimize deviations at constant pwm duty cycle values. High pwm switching frequencies increase the energy losses resulting in a lower driving voltage range, which reduces the effective range of selection for pwm duty cycle setting of flow rate adjustment. 1 kHz PWM frequency combined with the slow-decay driving mode achieves good performance in terms of linear regression and wider range for pwm duty cycle to flow rate transformation.

Keywords: PMDC Centrifugal Pump, Flow Regulation, Pwm Motor Control, Water Meter Test System.

Birleşik Tanklı Su Sayacı Test Sisteminde Geribeslemeli Doğrusallaştırma Tabanlı Santrifüj Pompa Akış Hızı Kontrolü

Öz

Daimi mıknatıslı doğru akım (PMDC) motorlu santrifüj pompası, geri besleme doğrusallaştırmalı birleştirilmiş tanklı su sayacı test sisteminde su besleme ünitesi olarak kullanılmak üzere tasarlanmıştır. Pompa tarafından üretilen akış hızı, bu tek girişli tek çıkışlı (SISO) sisteme giriş-çıkış geri besleme doğrusallaştırmasını uygulamak için gerekli giriş değişkenine karşılık gelmektedir. Pompa motoru, darbe genişlik modülasyonu (PWM) stratejisini çeşitli frekanslarda ve pwm yöntemlerinde uygulayan Arm Cortex M7 tabanlı bir mikro denetleyici tarafından yönetilmektedir. İstenilen görev döngüsü değerlerinde kararlı bir akış hızı sağlamak için en uygun pwm frekansı ve sürüş yönteminin belirlenmesi amaçlanmaktadır. Pompa motorunu sürmek için hem hızlı hem de yavaş düşme modlarında bir H-Bridge sürücü entegre devresi (L298N) kullanılmıştır. Debi ölçümleri, her mod için 100 Hz ile 20 kHz arasındaki 4 frekans değerinde gerçekleştirilmiştir. Düşük pwm frekansında (100 Hz) hızlı düşme modu, kararlı durumdaki su akış hızında daha fazla sapmalara neden olmaktadır. Yavaş düşme modunda ise, motor akımının daha yavaş azalmasına rağmen motor dönüş hızında frenleme etkisi ile daha hızlı bir azalma sağlamakta, bu da pompanın akış hızı stabilitesini iyileştirmekte ve arzu edilen pwm görev döngüsü değerlerinde sapmaları istenildiği şekilde en aza indirmektedir. Buna karşın, pwm anahtarlama frekansı arttırıldıkça, enerji kayıpları da arttığı için sürücünün kontrol edilebildiği gerilim aralığı azalmaktadır. Sonuç olarak 1 kHz Pwm frekansı, yavaş düşmeli sürüş moduyla birleştirildiğinde, doğrusal regresyon başarısı ve geniş kontrol edilebilme aralığı açısından en iyi performans elde edilmiştir.

Anahtar Kelimeler: PMDC Santrifüj Pompa, Akış Düzenleme, Pwm Motor Kontrolü, Su Sayacı Test Sistemi.

[*] Bahadır Yeşil: İzmir Katip Çelebi Üniversitesi, Fen Bilimleri Enstitüsü, Elektrik-Elektronik Mühendisliği Ana Bilim Dalı, İzmir, Türkiye, (ORCID: 0000-0002-9622-2593), b.yesil@baylanwatermeters.com

1. Introduction

Smart electronic meters that accurately measure water, electric and gas consumption are the main interest areas of internet of things implementations. In addition to the high-accuracy measurement features of smart meters, communication capabilities in various technology infrastructures are also available. These meters can store and transmit the consumption data repeatedly in a preconfigured period (Ramos et al., 2019). The ultrasonic water meter segment becomes the fastest growing smart liquid metering market in terms of meter physical type and measurement technology. Many researchers focus on this technology, for the reason that ultrasonic meters provide more precise and accurate flow values than mechanically constructed water meters. Santhosh & Roy (2012) introduced a brilliant flow measurement approach by using optimized neural network model on an ultrasonic flow meter. Hamouda et al. (2016) proposed a new method for measuring ultrasonic transit time difference with a precision as low as 10 picoseconds. Least-square-sine-fitting principle was used on the steady state receive signals at upstream and downstream directions which opened a new door in low flow rate measurement field. Lee et al. (2017) proposed a time of flight (TOF) type ultrasonic water meter that is applicable to residential water consumption measurement in low-to-medium flow rates. Suñol et al. (2018) presented the cross-correlation method for high precision TOF measurement in order to measure lower flow rates than other methods used in the metering industry. Since very low flow values can be measured in new generation meters, both the efficiency of water companies increases, and subscribers are directed towards better management of their own water consumption. Therefore, the choice of correct meter type plays an important role in preventing water losses.

As smart water meters enter our lives, their production processes and efficiency gain more importance. The test and calibration processes of these meters which have the ability to measure very low flow rates starting at 1 l/h require long cycle times and reduce the efficiency of industrial production line. Therefore, finding alternative solutions to traditional production and test systems is an important research and development area. Dutta & Komar (2017) stated two major drawbacks of conventional calibration techniques for smart water meters as time consuming process and exact dependency on the test system parameters. Any change in the pipe diameter, temperature or pressure at the system requires recalibration at full scale of input range. High precision and time saving methods are essential to be adapted to water meter test systems.

Flow-controlled variable speed water pumps are frequently used in industrial applications. Pumps with high power and high flow capacity are generally centrifugal and the flow rate of the pump is adjusted with frequency control. Since the flow rate in centrifugal pumps is directly proportional to the impeller speed, the control process is easier than other pump types. Janevska (2013) stated the linear mathematical model of a centrifugal pump system by using state variables method to describe the dynamics of the system. Goppelt et al. (2018) modeled a simple theoretical centrifugal pump system based on using lumped parameters, they showed that the centrifugal pump system could be modeled with a linear first order transfer function depending on the needed model accuracy. Shablovskiy & Kutoyov (2019) showed that pressure characteristic of a small pump can be considered as linear using the hydrodynamic modeling method and approximations. Applications which require steady flow rates can be implemented by using conventional PMDC motor based centrifugal pumps together with advanced control techniques.

Gevorkov et al. (2018) simulated and analyzed a pump model in Simulink for a wide range of flow settings, which can be used for working on various control methods of centrifugal pump constructions. Ivanov & Erkaev (2021) constructed a mathematical model of centrifugal pump based on calculations in ANSYS Fluent software. Gogolyuk et al. (2004) modeled a pump together with a synchronous motor by using the electrical analogy equivalent diagram of centrifugal pump. Naresh et al. (2012) modeled and simulated the PMDC pumping system fed by solar cell. Wang et al. (2021) established a mathematical model by using the basic parameters of the pump. In a different approach, A Aly (2007) studied a pump and dc motor system as a black box, applying Neural Network based on the conventional PID controller.

2. Material and Method

In order to apply feedback linearization based nonlinear control strategy to a coupled-tank water meter test bench, it is necessary to obtain exact system parameters to achieve best results. Flow rate corresponds to the input variable for such a single-input-single-output (SISO) system. It is mandatory to define input parameter correctly in the transformations to be applied for the input-output feedback linearization. The volumetric flow is transferred from the pump outlet directly to the first tank, so the inlet flow rate of the coupled tank system is directly proportional to the pump's rotational speed.

A PWM controlled pump is used to supply water to the 1st tank, so that the 2nd tank is not affected by the irregular flow caused by the pump dynamics. Feedback linearization method is used for controlling the water level h_2 at the 2nd tank (Figure 1). Calculation of the change of water level in the tank is implemented by using the principle of conservation of mass, which is based on the change of mass in the tank. The dynamic change is proportional to the difference between masses of water entering and leaving the tank, in terms of internal cross-sectional area:

$$A_1 \frac{dh_1}{dt} = Q_1 - Q_2$$

$$A_2 \frac{dh_2}{dt} = Q_2 - Q_3 - k_{bv} Q_4$$

At equilibrium, flow coefficient of the ball valve kbv is at preset value, and due to the constant water level set point, the derivatives of the water height in each tank must be zero.

$$u_1 = Q_1 = k_{PWM} w_{max,}\, u_2 = s_4, y_1 = h_2$$

$$Q_2 = s_2 a_2 \sqrt{2g(h_1 - h_2)}$$

$$Q_3 = s_3 a_3 \sqrt{2gh_2}$$

$$y_2 = Q_4 = k_{bv} * s_4 a_4 \sqrt{2gh_2}$$

Given as $h_1(t)$ and $h_2(t)$ are the water levels in the 1st and 2nd tanks respectively. $Q_1(t)$ is the inlet flow rate, $Q_2(t)$ is the flow rate between two tanks, $Q_3(t)$ is the stabilization flow rate from 2nd tank to reservoir, and $Q_4(t)$ is the flow rate from 2nd tank to test

bench which is turned on during water meter test. The cross-sectional areas of the tanks are given as A_1 and A_2, and the orifice areas of the inlets and outlets of the tanks given with the flow coefficients for Q_2, Q_3 and Q_4 as s_2a_2, s_3a_3 and s_4a_4, respectively. The system is defined by the following nonlinear differential equations:

$$\frac{dh_1}{dt} = \frac{1}{A_1}(k_{PWM}w_{max}u_1 - s_2a_2\sqrt{2g(h_1 - h_2)})$$

$$\frac{dh_2}{dt} = \frac{1}{A_2}(s_2a_2\sqrt{2g(h_1 - h_2)} - s_3a_3\sqrt{2gh_2} - k_{bv} * s_4a_4\sqrt{2gh_2})$$

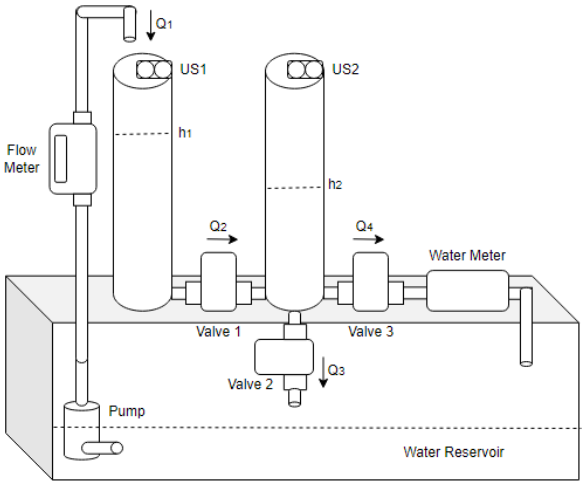

Figure 1. Block Diagram of Modeled System

By defining state variables as $x_1 = h_2$ and $x_2 = h_1 - h_2$, dynamic model of the meter test bench is obtained, and state equations can be given as:

$$\dot{x_1} = \frac{dh_2}{dt} = -\frac{(s_3a_3 + k_{bv} * s_4a_4)\sqrt{2g}}{A_2}\sqrt{x_1} + \frac{s_2a_2\sqrt{2g}}{A_2}\sqrt{x_2}$$

$$\dot{x_2} = \frac{(s_3a_3 + k_{bv} * s_4a_4)\sqrt{2g}}{A_2}\sqrt{x_1} - \frac{(A_1 + A_2)s_2a_2\sqrt{2g}}{A_1A_2}\sqrt{x_2} + \frac{k_{PWM}w_{max}}{A_1}u$$

$$y = h_2 = x_1$$

In order to obtain the relative degree of output in proposed system, output is differentiated repeatedly until the input variable appears explicitly in the result:

$$\dot{y} = \frac{dh(x)}{dt} = \frac{\partial h(x)}{\partial x} * \frac{dx}{dt} = \frac{\partial h(x)}{\partial x} * \dot{x}$$

By using the functional representation of the dynamic model:

$$\dot{x} = f(x) + g(x) * u$$

Differentitation of the output can be simplified in terms of Lie derivatives of h(x) with respect to f and g:

$$\dot{y} = \frac{\partial h(x)}{\partial x} * [f(x) + g(x) * u] = L_fh(x) + L_gh(x) * u$$

The first derivative of the output is equal to the state equation $\dot{x_1}$ of the system, which does not include an input term in it:

$$\dot{y} = \dot{x_1} = \frac{dh_2}{dt} = -\frac{(s_3a_3 + k_{bv} * s_4a_4)\sqrt{2g}}{A_2}\sqrt{x_1} + \frac{s_2a_2\sqrt{2g}}{A_2}\sqrt{x_2}$$

Therefore $\dot{y}$ is independent of u. In terms of Lie derivative:

$$L_gh(x) = 0 \; and \; \dot{y} = L_fh(x)$$

Taking the second derivative of the output results in a form which includes both state equations $\dot{x_1}$ and $\dot{x_2}$:

$$y^{(2)} = x_1^{(2)} = -\frac{(s_3a_3 + k_{bv} * s_4a_4)\sqrt{2g}}{A_2 * 2\sqrt{x_1}}\dot{x_1} + \frac{s_2a_2\sqrt{2g}}{A_2 * 2\sqrt{x_2}}\dot{x_2}$$

After substituting the state equations into $y^{(2)}$ and simplifying them:

$$y^{(2)} = \frac{2gs_2a_2(s_3a_3 + k_{bv} * s_4a_4)}{2A_2^2}\left(\frac{\sqrt{x_1}}{\sqrt{x_2}} - \frac{\sqrt{x_2}}{\sqrt{x_1}}\right) + \frac{2g(s_3a_3 + k_{bv} * s_4a_4)^2}{2A_2^2} - \frac{2g(s_2a_2)^2(A_1 + A_2)}{2A_1A_2^2} + \frac{s_2a_2\sqrt{2g}}{2A_1A_2}\frac{k_{PWM}w_{max}}{\sqrt{x_2}}u$$

Input is obtained in the 2nd derivative, so the relative degree of the output is 2. The proposed system is fully feedback linearizable, because the relative degree of the output is equal to the order of the system.

$$k = n = 2, y^{(2)} = L_f^2h(x) + L_gL_fh(x) * u, y^{(2)} = v$$

A transformation is implemented in order to form a linear system with the new input v:

$$\dot{z_1} = z_2, \dot{z_2} = v, y = z_1$$

$$\dot{z} = \begin{bmatrix} 0 & 1 \\ 0 & 0 \end{bmatrix} z + \begin{bmatrix} 0 \\ 1 \end{bmatrix} v$$

$$y = [1 \quad 0]z$$

$$y^{(2)} = v = f(x) + \Phi(x) * u$$

$$f(x) = \frac{2gs_2a_2(s_3a_3 + k_{bv} * s_4a_4)}{2A_2^2}\left(\frac{\sqrt{x_1}}{\sqrt{x_2}} - \frac{\sqrt{x_2}}{\sqrt{x_1}}\right) + \frac{2g(s_3a_3 + k_{bv} * s_4a_4)^2}{2A_2^2} - \frac{2g(s_2a_2)^2(A_1 + A_2)}{2A_1A_2^2}$$

$$\Phi(x) = \frac{s_2a_2\sqrt{2g}}{2A_1A_2}\frac{k_pw_{max}}{\sqrt{x_2}}$$

Here, u is the original input to the nonlinear system. Simply by taking it to the left side of the equation, it can be defined in terms of new input of the system v and non linear states:

$$u = \frac{v - f(x)}{\Phi(x)}$$

Finally the original input u can be stated as:

$$= \frac{2A_1A_2^2v - (2A_1gs_2a_2(s_3a_3 + k_{bv} * s_4a_4))\left(\frac{\sqrt{x_1}}{\sqrt{x_2}} - \frac{\sqrt{x_2}}{\sqrt{x_1}}\right)}{\frac{A_1s_2a_2\sqrt{2g}}{1}\frac{k_pw_{max}}{\sqrt{x_2}}} + \frac{2A_1g(s_3a_3 + k_{bv} * s_4a_4)^2 - 2g(s_2a_2)^2(A_1 + A_2)}{\frac{A_1s_2a_2\sqrt{2g}}{1}\frac{k_pw_{max}}{\sqrt{x_2}}}$$

Which means that, if the input flow rate from the centrifugal pump is applied as $u = \frac{1}{\Phi}(-f + v)$ to the proposed system where v is the new input, then the nonlinearity is avoided. So, a simple relationship is obtained between output and new input v:

$$y^{(2)} = v$$

2.1. Experimental Setup

Experimental setup consists of a flow generator submersible pump and a frequency-output reference flow meter connected to the embedded control system of coupled tank (Figure 2), which communicates with PC via serial port.

2.1.1. Main Control Unit

Arm Cortex M7 32-Bit Microcontroller is used for the control system, which operates at 216 MHz with FPU support for complex mathematical operations. A high-resolution TFT display is used in the embedded control system to provide a clear, instantaneous display of variables in the experiments (Figure 3). Pwm signal generation is implemented by the internal general purpose timer, which works in non-blocking mode without interrupting the cpu during the state transitions of duty cycle. Duty cycle change is executed in the PWM on-the-fly mode without blocking the cpu and not requiring time-delay for peripheral init – deinit operations. STM32F7-Discovery board is connected to the PC via USB serial port, which is used as both debugging and virtual com port. Virtual com port is used for obtaining flow rate information to the PC through a serial port terminal application during real time running mode. Cortex-M7 processor with 216MHz CPU speed, full duplex Uart and I/O configurable Timer with Direct Memory Access (DMA) controller form the basis of the main hardware layer.

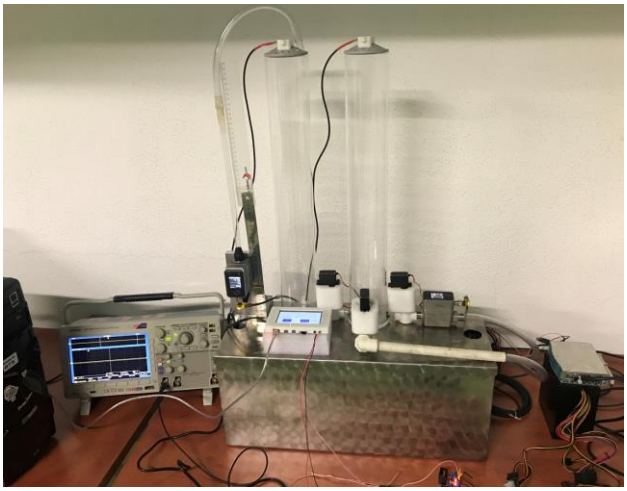

Figure 2. Photo of Experimental Setup

Non-blocking coding method is implemented in the bare-metal control firmware. Serial communication (UART) port is initialized in DMA mode and connected to the PC through the virtual com port of debugger. Direct memory access capability eliminates the need for the CPU for transmitting the measured data to the PC. Any other methods i.e. input polling or interrupt relies on CPU operations to stop by and execute communication, conversely the DMA functionality releases the CPU for other tasks completely.

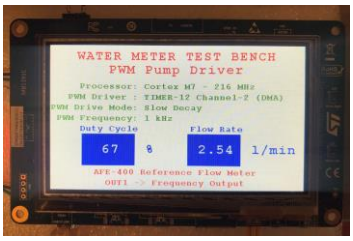

(a) *(b)*

Figure 3. Main Control Unit Display (a), STM32F7 Discovery Board (b)

2.1.2. Motor Pump

Water meter test system requires a constant flow rate during the test cycle. When the flow is supplied directly by the pump, internal dynamics of pump motor and small variations in the impeller angular frequency cause flow disturbances which reduces the accuracy and reliability of the measurement system. Instead of direct feeding the meter under test, coupled-tank drain method is studied to generate a constant flow. Therefore, a pwm controlled pump is used to supply water to the first tank of coupled system, so that the second tank is not affected by the irregular flow caused by the pump dynamics (Figure 5).

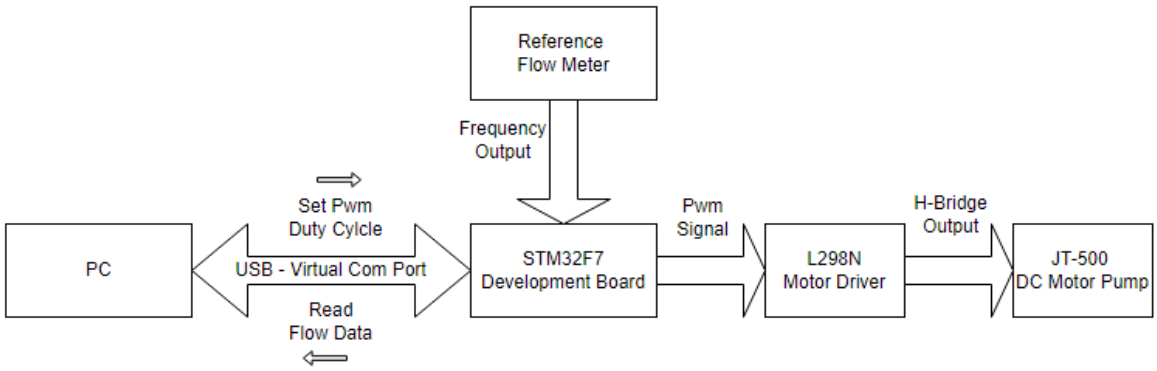

Figure 4. Control System Block Diagram

DC Brushed Motor pump is driven by the pwm signal generated from an embedded Arm Cortex M7 microcontroller development platform. Logical drive signal is amplified and applied to the motor pump by using an integrated H-bridge driver circuit. The effect of pwm frequency over the relationship between the duty cycle and flow rate is explored in this study. Both outputs of the L298N dual H-bridge driver circuit are connected and used in parallel as a single H bridge output, in order to increase the maximum drive current from 2A to 4A. PWM voltage at 100% duty cycle is applied as +12V DC (which is the nominal operating voltage of the DC pump, and will be defined as the input voltage value at maximum flow rate).

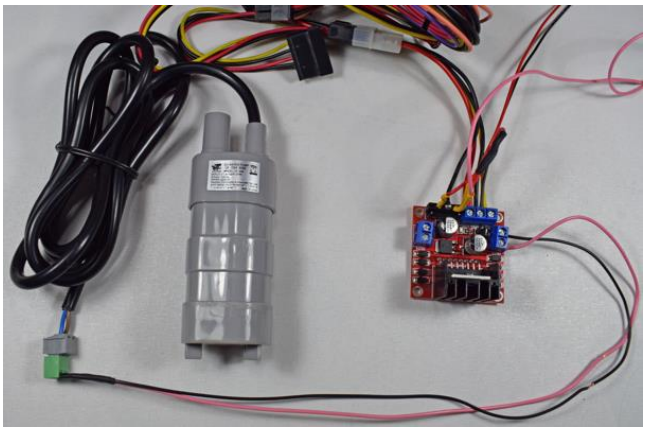

Figure 5. PMDC Motor Pump and L298N Driver Module

DC motor pump is supplied by the H-Bridge Motor driver with 4 different pwm signals selected from 100 Hz to 20 kHz. For each frequency value, generated pulse width is adjusted from 10% to 100% with each step of 1 percentage by the controller software. Total dynamic pump head and the flow rate is recorded at each step. As a rule of thumb, the flow rate does not start until the pump head reaches to the height of the U-shaped flow pipe.

2.1.2. Reference Flow Meter

An electromagnetic flow meter is used as reference flow measurement unit in the experimental setup (Figure 6). Flow rate is obtained from the frequency output of the reference flow meter, which is connected to the timer/counter input of the microcontroller through a system clock prescaler. Measurement range and flow output frequency are configured according to the physical limit of the maximum pump flow which is equal to 10 l/min.

Figure 6. Flow Meter Connection

2.1.2. H-Bridge Pump Motor Driver

H-Bridge circuits are mainly used in motor drivers, inverter circuits and new generation battery charging devices for electrical vehicles. Gupta (2010) presented three alternative circuits of H-Bridge for driving a DC motor, with comparison in terms of current consumption and efficiency. Mori et al. (2016) worked on a new strategy to reduce high-frequency harmonics by modifying the slope of transients during switching in a step-down converter which is designed with H-Bridge. Drgona & Stefun (2018) studied the application of stepper motors with H-bridge drivers in CNC machines. El-Saadawi et al. (2020) modeled a DC motor and applied fractional order PID for speed control through L298N H-bridge motor driver using fast decay mode. In this study, H-Bridge circuit of L298N is activated with a general “ENABLE” port which drives one input of each AND Gate to logic high. The other input of each AND gate is driven by the IN1 and IN2 ports. As the rotation of the pump should be always in the same direction, IN2 port is tied to ground - logic low. Driving the pump by switching the Enable port causes all the Gates to be disabled during pwm low cycles (signal path 2 in Figure 7), which generates a fast decay mode. On the other hand, switching the IN1 port keeps the low side Gates activated and a slow decay mode is observed (signal path 3 in Figure 7).

2.1.3. Test and Measurement

First, L298N motor driver circuit is first configured to work in fast decay mode with the command sent from the computer. (IN1 input port is hold at logic high level, pwm signal is applied to ENABLE A port.) In fast decay mode, pwm duty cycle is increased by one percent starting from 1% for 5 seconds measurement at each frequency value. 5 samples were taken from the reference measuring instrument where the flow rate is

calculated within 1 second intervals. This is implemented by the timer/counter peripheral of the microcontroller by setting to 1 second overflow value to count the pulses received from the frequency output of the reference meter within this period. Total 5*100 samples were obtained at each frequency value up to 100% pwm duty cycle. The mean and standard deviation of the obtained samples are calculated and given in table-3 by multiples of 10 percent.

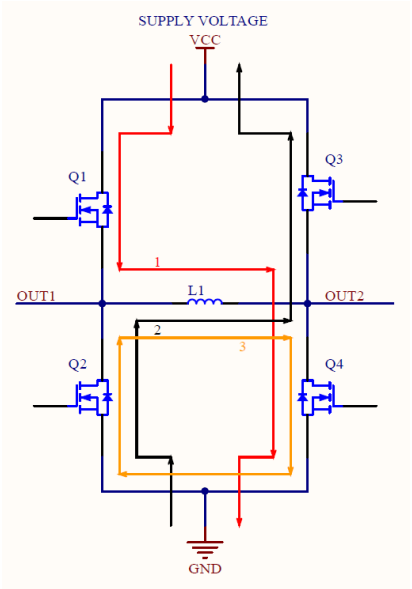

Figure 7. Fast and Slow Decay Mode Current Paths in a H-Bridge Driver

Subsequently, switching to the slow decay mode command was sent to the drive circuit where the remaining test conditions were kept unchanged, and samples were taken again. (ENABLE A port is hold at logic high level and the pwm signal is applied to the IN1 input port of the motor driver). The mean and standard deviation of new samples are given in table-4.

3. Results and Discussion

Fast decay mode and slow decay mode current paths are shown in Figure 7. In fast decay mode, reverse current flows through Q_2 and Q_3 transistors, related current path is given in black colour. Fast decay mode in low pwm frequencies (100 Hz – 1 kHz) has more deviations in the flow rate at constant duty cycle values. In slow decay mode, both transistors at the low side (Q_2 and Q_4) are still active during the pwm signal off cycles. This current path through Q_2 and Q_4 results in a slower decay in current, which causes a rapid decrease in the motor speed. Slow decay mode provides better performance in terms of efficiency and stable flow at these frequency levels. At higher range pwm frequencies (10 kHz – 20 kHz), decay mode does not affect the overall performance of the flow supply system. However, high pwm switching frequencies increase the energy losses resulting in a lower driving voltage range, similar to the findings of Van Der Geest et al. (2014) that investigated the losses in the rotor, windings and laminations of a permanent magnet machine caused by the PWM switching frequency.

Table 3. Fast Decay Mode Flow Characteristics (ENABLE_A=1, pwm signal applied to IN1)

	PWM Frequency							
	100 Hz		1 kHz		10 kHz		20 kHz	
Duty Cycle (%)	Water Height (cm)	Flow Rate (l/min)	Pump Head (cm)	Flow Rate (l/min)	Pump Head (cm)	Flow Rate (l/min)	Pump Head (cm)	Flow Rate (l/min)
10	0	0	0	0	0	0	0	0
20	0	0	0	0	0	0	0	0
30	29.0±1.8	0	16.3±0.5	0	0	0	0	0
40	56.5±1.4	0	45.0±0.3	0	9.0±0.4	0	9.5±0.3	0
50	66.5	0.96±0.04	66.5	0.45±0.02	35.5±0.3	0	39.0±0.2	0
60	66.5	2.14±0.06	66.5	1.78±0.02	66.5	0.31±0.01	66.5	0.35±0.02
70	66.5	3.17±0.10	66.5	2.81±0.03	66.5	2.02±0.02	66.5	2.07±0.03
80	66.5	3.99±0.08	66.5	3.59±0.02	66.5	3.29±0.02	66.5	3.31±0.02
90	66.5	4.69±0.09	66.5	4.40±0.02	66.5	4.25±0.03	66.5	4.22±0.03
100	66.5	5.20±0.10	66.5	5.12±0.02	66.5	5.13±0.01	66.5	5.12±0.02

Radsanjani & Astharini (2017) studied control application of a DC motor, and compared the results at different frequency levels presenting an efficient range between 400 and 600 Hz in their setup, while the experiments in this research give out optimum performance at 1 kHz as the dc motor is coupled to the pump.

Maximum driving voltage (100% duty cycle) is DC 12V. Due to the internal physical construction of permanent magnets and coils of DC motor, rotation starts after 24% pwm duty cycle which is equal to an average driving voltage of 2.88V. Regardless of the pwm frequency, lower voltage levels at duty cycle less than 24% can not deliver adequate current to the motor coils resulting an insufficient electromagnetic force, so the motor does not start to rotate.

4. Conclusions and Recommendations

PMDC motor centrifugal pump is driven by an Arm Cortex M7 based microcontroller applying the PWM method at different frequencies and driving modes. Flow rate measurements are carried out at 100 Hz, 1 kHz, 10 kHz and 20 kHz for each mode. Fast decay mode in low pwm frequency (100Hz) results in higher deviations which is not the optimum setting for a regular flow supply. Better than this setting, slow decay mode provides a faster reduction in motor speed despite the slower current decay, which improves the flow rate stability and minimize deviations at constant pwm duty cycle values. However, high pwm switching

frequencies reduces the effective range of selection for pwm duty cycle setting of flow rate adjustment.

1 kHz Pwm frequency in slow-decay driving mode achieved leading performance within 4 frequency (100Hz, 1kHz, 10kHz, 20kHz) values and 2 decay (fast, slow) modes, in terms of improved linearization and wider range for pwm duty cycle to flow rate transformation. This setting assures exact knowledge of dynamic input parameter (Q_1) for feedback linearization.

Internal floating point unit availability and high CPU speed (up to 216MHz) of Cortex M7 microcontroller used in the experiments are highly sufficient for medium-to-large scale control applications. Compatibility with the other microcontrollers in the same family of Arm Cortex Mx Core allows a wide spectrum of applications without changing the main controller design concept. State feedback and coordinate transformation algorithms for feedback linearization and advanced control strategies of complex non-linear systems can be implemented on-board without the processing support of additional high-performance computers.

Table 4. Slow Decay Mode Flow Characteristics (IN1=1, pwm signal applied to ENABLE_A)

	PWM Frequency							
	100 Hz		1 kHz		10 kHz		20 kHz	
Duty Cycle (%)	Water Height (cm)	Flow Rate (l/min)	Pump Head (cm)	Flow Rate (l/min)	Pump Head (cm)	Flow Rate (l/min)	Pump Head (cm)	Flow Rate (l/min)
10	0	0	0	0	0	0	0	0
20	0	0	0	0	0	0	0	0
30	28.5±0.5	0	16.0±0.3	0	0	0	0	0
40	55.0±0.3	0	44.8±0.2	0	9.0±0.3	0	9.5±0.3	0
50	66.5	0.95±0.01	66.5	0.44±0.01	35.5±0.3	0	39.0±0.1	0
60	66.5	2.11±0.02	66.5	1.76±0.01	66.5	0.30±0.01	66.5	0.34±0.01
70	66.5	3.10±0.02	66.5	2.80±0.02	66.5	2.02±0.02	66.5	2.06±0.02
80	66.5	3.85±0.01	66.5	3.60±0.01	66.5	3.28±0.02	66.5	3.29±0.02
90	66.5	4.48±0.02	66.5	4.37±0.02	66.5	4.26±0.03	66.5	4.21±0.02
100	66.5	5.15±0.03	66.5	5.10±0.01	66.5	5.14±0.01	66.5	5.12±0.01

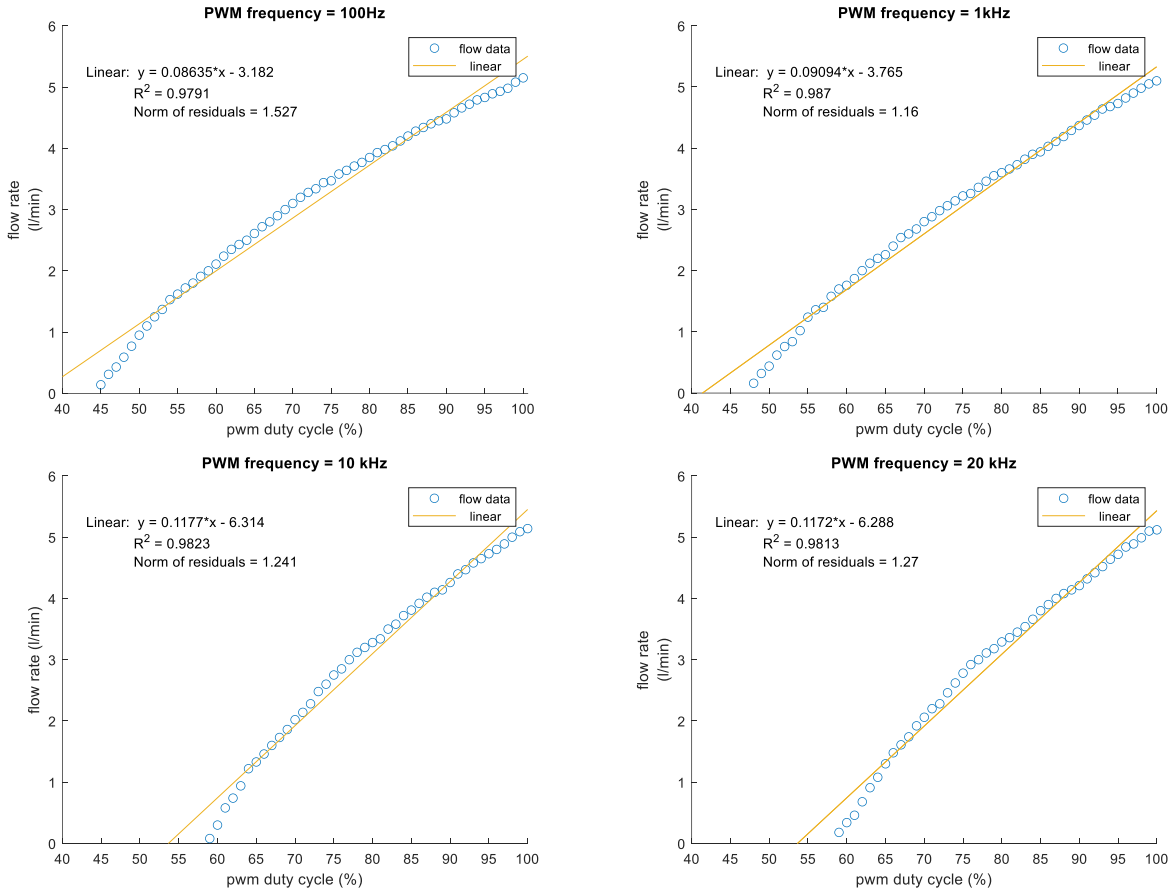

Figure 8 - Linearity Evaluation Between Duty Cycle and Flow Rate at Different Frequencies

References

A Aly, A. (2007). Flow rate control of variable displacement piston pump with pressure compensation using neural network. *JES. Journal of Engineering Sciences*, *35*(6), 1401-1412.

Drgona, P., & Stefun, R. (2018, October). Application of Stepper Motors in CNC Device. In *2018 International Conference and Exposition on Electrical And Power Engineering (EPE)* (pp. 241-246). IEEE.

Dutta, P., & Kumar, A. (2017). Intelligent calibration technique using optimized fuzzy logic controller for ultrasonic flow sensor. *Mathematical Modelling of Engineering Problems*, *4*(2), 91-94.

El-Saadawi, M. M., Gouda, E. A., Elhosseini, M. A., & Essa, M. S. (2020). Identification and Speed Control of DC Motor Using Fractional Order PID: Microcontroller. *European Journal of Electrical Engineering and Computer Science*, *4*(1).

Gevorkov, L., Rassõlkin, A., Kallaste, A., & Vaimann, T. (2018, January). Simulink based model for flow control of a centrifugal pumping system. In *2018 25th International Workshop on Electric Drives: Optimization in Control of Electric Drives (IWED)* (pp. 1-4). IEEE.

Gogolyuk, U., Lysiak, V., & Grinberg, I. (2004, October). Mathematical modeling of a synchronous motor and centrifugal pump combination in steady state. In *IEEE PES Power Systems Conference and Exposition, 2004.* (pp. 1444-1448). IEEE.

Goppelt, F., Hieninger, T., & Schmidt-Vollus, R. (2018, December). Modeling centrifugal pump systems from a system-theoretical point of view. In *2018 18th International Conference on Mechatronics-Mechatronika (ME)* (pp. 1-8). IEEE.

Gupta, V. (2010, March). Working and analysis of the H-bridge motor driver circuit designed for wheeled mobile robots. In *2010 2nd International Conference on Advanced Computer Control* (Vol. 3, pp. 441-444). IEEE.

Hamouda, A., Manck, O., Hafiane, M. L., & Bouguechal, N. E. (2016). An enhanced technique for ultrasonic flow metering featuring very low jitter and offset. *Sensors*, *16*(7), 1008.

Janevska, G. (2013, September). Mathematical modeling of pump system. In *Electronic International Interdisciplinary Conference* (No. September 2013, pp. 455-58).

Ivanov, V. A., & Erkaev, N. V. (2021). Numerical and analytical modeling of centrifugal pump.

Lee, C. H., Jeon, H. K., & Hong, Y. S. (2017). An implementation of ultrasonic water meter using dToF measurement. *Cogent Engineering*, *4*(1), 1371577.

Mori, T., Funato, H., Ogasawara, S., Okazaki, F., & Hirota, Y. (2016). Improved Modified Switching Transient Pulse Width Modulation (MT-PWM) Method Applied to H-Bridge Type Step-Down Converter. *Electrical Engineering in Japan*, *194*(3), 59-69.

Naresh, B., Madhu, P., & Prasad, K. R. K. (2011). Analysis of DC solar water pump and generalized photovoltaic model using Matlab/Simulink. *UACEE International Journal of Advancements in Electronics and Electrical Engineering*, *1*(1).

Radsanjani, M. F., & Astharini, D. (2018). PC Based Real Time Control of DC Motor. *Jurnal Al-Azhar Indonesia Seri Sains dan Teknologi*, *4*(2), 66-69.

Ramos, H. M., McNabola, A., López-Jiménez, P. A., & Pérez-Sánchez, M. (2019). Smart water management towards future water sustainable networks. *Water*, *12*(1), 58.

Santhosh, K. V., & Roy, B. K. (2012). An intelligent flow measurement technique using ultrasonic flow meter with optimized neural network. *International journal of control and automation*, *5*(4), 185-195.

Shablovskiy, A., & Kutovoy, E. (2019, March). Obtaining the head characteristic of a Low Flow Centrifugal Pump by numerical methods. In *IOP Conference Series: Materials Science and Engineering* (Vol. 492, No. 1, p. 012035). IOP Publishing.

Suñol, F., Ochoa, D. A., & Garcia, J. E. (2018). High-precision time-of-flight determination algorithm for ultrasonic flow measurement. *IEEE Transactions on Instrumentation and Measurement*, *68*(8), 2724-2732.

Van Der Geest, M., Polinder, H., & Ferreira, J. A. (2014, September). Influence of PWM switching frequency on the losses in PM machines. In *2014 International Conference on Electrical Machines (ICEM)* (pp. 1243-1247). IEEE.

Wang, Y., Zhang, H., Han, Z., & Ni, X. (2021). Optimization design of centrifugal pump flow control system based on adaptive control. *Processes, 9*(9), 1538.